Journal of Alloys and Compounds 509S (2011) S562–S566

Contents lists available at ScienceDirect

Journal of Alloys and Compounds

journal homepage: www.elsevier.com/locate/jallcom

Catalytic effect of fullerene and formation of nanocomposites with complex hydrides: $NaAlH_4$ and $LiAlH_4$

Joseph A. Teprovich Jr., Douglas A. Knight, Matthew S. Wellons, Ragaiy Zidan*

Savannah River National Laboratory, Aiken SC, 29801 United States

ARTICLE INFO

Article history:
Received 31 August 2010
Received in revised form 6 October 2010
Accepted 7 October 2010
Available online 15 October 2010

Keywords:
Hydrogen storage
Complex hydrides
Fullerene

ABSTRACT

Carbonaceous nanomaterials utilized as scaffolds, catalysts, and additives in conjunction with complex metal hydrides have shown remarkable hydrogen sorption properties. Our studies have confirmed fullerene-C_{60} is an excellent catalyst for temperature induced hydrogen desorption for both $NaAlH_4$ and $LiAlH_4$. Fullerene-containing complex metal hydride composites comprised of fullerene-C_{60} with $NaAlH_4$ or $LiAlH_4$ desorbed hydrogen at elevated temperature and go onto form alkali metal fullerides and aluminum metal as final products. The as-prepared composites exhibit rapid hydrogen desorption at onset temperatures of 130 °C and 150 °C, and released hydrogen content of 5.9 and 2.2 wt.% ($LiAlH_4$ and $NaAlH_4$, respectively) relative to the composite. The resultant alkali metal fulleride containing composites have been characterized and are capable of reversible hydrogen storage. A series of desorption/absorption experiments on the Na–C_{60} and Li–C_{60} based composites demonstrate a 1.5 wt.% and a 1.2 wt.% reversible capacity, respectively. The complex metal hydride-C_{60} systems were characterized by PCT, XRD, FT-IR, and TGA-RGA and demonstrate the formation of fulleride material similar to traditional hydrofullerenes which appear to be responsible for the observed reversible hydrogen storage.

1. Introduction

Previous work from our group has examined the catalytic properties of carbonaceous materials on the reversible hydrogen storage properties of complex hydrides, $LiBH_4$ and $NaAlH_4$ [1,2]. Extending this motif, we have expanded our investigation of the hydrogen storage properties of C_{60}–$NaAlH_4$ and C_{60}–$LiAlH_4$ composites. Both $NaAlH_4$ and $LiAlH_4$ are well studied complex hydrides with desirable practical hydrogen capacities (5.5 and 7.9 wt.%, respectively) and were targets of this investigation [3–6]. We were able to intimately mix both complex hydrides with fullerene, via solvent assisted mixing [1,2], forming a homogeneous composite which desorbs hydrogen gas at elevated temperature, and the resultant composite is capable of reversible hydrogen absorption/desorption.

Several groups have investigated the use of carbon materials as possible catalysts for various complex hydrides (in particular $NaAlH_4$) and samples are prepared either by ball milling [7–11] or melt infiltration [12–14]. All these groups report that carbon materials act as catalysts for hydrogen sorption of $NaAlH_4$. The catalytic effect is believed to be either through nano-sizing or closer contact with carbon nanostructures. Past research on $LiAlH_4$ has been aimed at lowering the temperature of desorption through either mechanical-milling and/or by the addition of transition metal additives [15–17]. More recent research has focused on regenerating $LiAlH_4$ through solvent-assisted methods due to the high lattice energy of Li_3AlH_6 [18–20]. However, there has not been an attempt made to examine the effect of carbon nanomaterials on the desoprtion/absorption properties of $LiAlH_4$. Fulleride materials have received scant attention as hydrogen storage media with only two published systems which include mixed anatase fulleride composites and a Pt-fulleride system [17,21].

Here we report the synthesis and detailed characterization of alkali metal fullerides capable of reversible hydrogen absorption/desorption. The materials are prepared by combination of a C_{60} additive and complex metal hydrides by a solvent preparation technique to intimately mix $NaAlH_4$ or $LiAlH_4$ with C_{60} without introducing metal contaminants. Since our study is focused on investigating the properties of carbon nanomaterials of particular shape and structure on hydrogen sorption, we used sample preparation techniques which *avoid* introduction of metal contaminants and degradation of the carbon nanostructures. Ball milling is known to degrade fragile carbon nanostructures [22,23] and is known to introduce Fe contamination from the ball mill vial and/or balls [16,24]. We present a combination of powder X-ray diffraction (XRD), infrared spectroscopy (IR), temperature programmed desorption (TPD), and coupled thermogravimetric residual gas analysis to demonstrate the reversible hydrogen storage of sodium fulleride at 1.5 wt.% and of lithium fulleride at 1.2 wt.%.

* Corresponding author. Tel.: +1 803 646 8876; fax: +1 803 652 8173.
E-mail address: ragaiy.zidan@srnl.doe.gov (R. Zidan).

0925-8388/$ – see front matter © 2010 Elsevier B.V. All rights reserved.
doi:10.1016/j.jallcom.2010.10.031

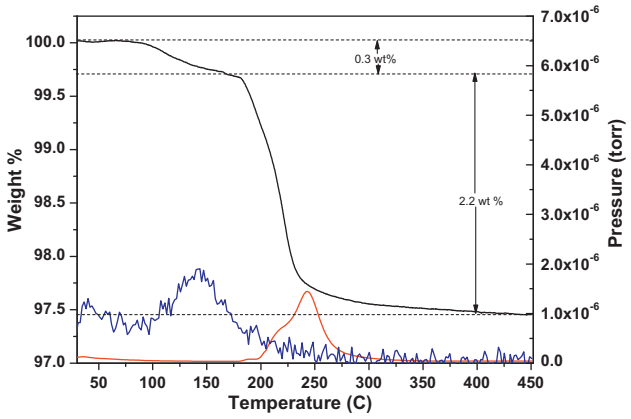

Fig. 1. TGA-RGA of the $NaAlH_4$:C_{60} composite (black) shows only a 0.3 wt.% loss due to benzene (blue). The RGA signal for benzene was multiplied × 500 to fit on the scale of the graph. Hydrogen (red) release corresponds to the weight loss observed in the TGA. (For interpretation of the references to colour in this figure legend, the reader is referred to the web version of the article.)

2. Materials and methods

Chemicals were used as provided by the supplier and are listed by supplier as follows. Acros: THF (anhydrous, ≥99.9%, inhibitor-free), Benzene (anhydrous). Sigma–Aldrich: C_{60} (99.5%), $LiAlH_4$ (95%), and $NaAlH_4$ (hydrogen storage grade). All chemicals were stored and handled under an argon atmosphere in a Vacuum Atmospheres glovebox.

Samples were prepared by combining fullerene and the respective complex metal hydride with either THF or benzene. The mixture was stirred with a Teflon™ coated magnetic stir bar for 12 h. The solvent was removed under reduced pressure and the remaining solids collected. The $LiAlH_4$ composite was prepared in a 60:1 mol ratio ($LiAlH_4$:C_{60}) which is equivalent to the composite containing 76 wt.% $LiAlH_4$. The sodium alanate ($NaAlH_4$) composite was prepared with a 6:1 ratio of Na:C_{60} using (6.0 mmol, 0.324 g) $NaAlH_4$ and (1.0 mmol, 0.720 g) C_{60} and stirring with 50 mL of benzene.

The hydrogen desorption/absorption properties of the material were measured on a HyEnergy PCT Pro 2000 instrument. The PCT vessel and sample were heated at a rate of 2 °C/min from room temperature (RT) to 300 or 380 °C followed with an isotherm, during which an increase in pressure attributed to the evolution of H_2 was observed. After desorption, the sample was evacuated and allowed to cool to RT before the absorption cycle was started. For the absorption the sample was first charged with 105–120 bar H_2, and then heated to 250 °C or 350 °C, followed by a 9–12 h isotherm. Subsequent reversible hydrogen cycling was conducted with identical parameters.

For TGA-RGA experiments a Perkin Elmer Thermogravimetric Analyzer-Pyris 1 TGA was used within an inert glovebox. The sample was heated from 30 to 550 °C at heating rate of 2–5 °C/min, with a sample size of ~5 mg. The gas released during the heating process was identified by a Hiden Analytical RGA. X-ray powder diffraction (XRD) was used to characterize the products, using Cu-K radiation. During X-ray analysis the samples were protected with a Mylar film to minimize oxidation. Samples analyzed by FT-IR were prepared as KBr pellets in an Argon glovebox and were analyzed on a Jasco FT-IR 6300 with a stream of nitrogen purging the sample chamber.

3. Results and discussion

3.1. $NaAlH_4$:C_{60} system

As an expansion on previous work the $NaAlH_4$:C_{60} system, sorption behavior was studied by observing the thermal sorption behavior on both the TGA-RGA and PCT. The resulting solids were then characterized using both FT-IR spectroscopy and X-ray powder diffraction [1]. The TGA-RGA results, shown in Fig. 1, indicates an as-prepared $NaAlH_4$:C_{60} (6:1) mixture undergoes a thermal decomposition in a temperature range similar to previous studies on $NaAlH_4$ where the complex hydride has been subjected to ball milling [8] or catalyzed [6–11,25]. The initial loss of 0.3 wt.% is the loss of trace amounts of benzene remaining from the composite solvent mixing process and is confirmed by RGA analysis. The decomposition of the $NaAlH_4$:C_{60} (6:1) occurs over a 180–230 °C temperature range with approximately a 2.2 wt.% loss indicative of a complete transition to Na, Al, C and hydrogen gas constituents. The final mass loss (i.e. hydrogen) can only be accounted for through the complete decomposition of the metal hydride into Na and Al metal and hydrogen. The final ~2.2 wt.% loss can be equated to the complete dehydrogenation of sodium alanate as in reaction (1):

$$NaAlH_4 \rightarrow Na + Al + 2H_2 \quad (1)$$

This mass loss is consistent with a calculated mass loss of 2.3 wt.% for an idealized 6:1 ($NaAlH_4$:C_{60}) composite which is completely dehydrided. The thermal decomposition of NaH at this low temperature is unprecedented with most $NaAlH_4$ hydrogen storage studies reporting NaH as the final product. Note that pure NaH within an inert atmosphere decomposes into Na metal and hydrogen above 400 °C.

As shown in Fig. 2, TPD measurements mirror the TGA-RGA data with a release of 2.2 wt.% hydrogen from the composite material during the first desorption; again indicative of a complete dehydriding of the $NaAlH_4$ composite component. The initial desorption of the as-prepared material is composed of two visible transitions starting at ~60 and ~250 °C and are likely due to reactions (2) and (3).

$$NaAlH_4 \rightarrow NaH + Al + 3/2H_2 \quad (2)$$

$$NaH \rightarrow Na + 1/2H_2 \quad (3)$$

For the 6:1 ($NaAlH_4$:C_{60}) composite, the idealized calculated desorption from NaH decomposition would be 0.5 wt.% hydrogen, which matches well with the evident second desorption inflection. The observed decrease in NaH dehydrogenation temperature could not be the result of catalytic activity alone due to the presence of the C_{60} additive. It is likely the result of the formation of Na/C_{60} composite which differs thermodynamically from pure NaH or C_{60}. It is important to point out the absence of the formation of Na_3AlH_6 as an intermediate in the presence of C_{60}. Na_3AlH_6 formation occurs during the dehydrogenation of pure $NaAlH_4$ or catalyzed with transition metals.

Post first desorption, the 6:1 material was charged with 120 bar H_2, heated to 250 °C followed by a 12 h isotherm at 250 °C. TPD measurements of the recharged material show a single desorption with onset temperature ~150 °C and a total 1.5 wt.% hydrogen desorption relative to the composite mass. This "partial" rehydrogenation/dehydrogenation of the composite mimicking the

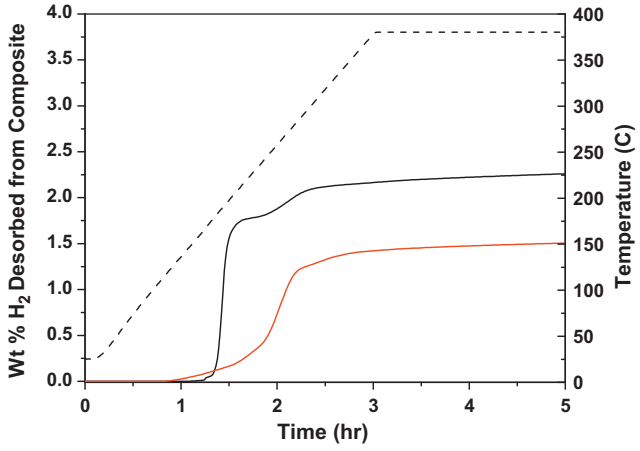

Fig. 2. The 1st (black) and 2nd (red) desorption of the $NaAlH_4$:C_{60} material is shown. The 1st desorption presents a wt.%. loss that indicates the dehydrogenation of the NaH occurs at a low temperature. The 2nd desorption shows this material's ability to exhibit a small amount of sorption reversibility. Sample temperature ramp is the dashed line. (For interpretation of the references to colour in this figure legend, the reader is referred to the web version of the article.)

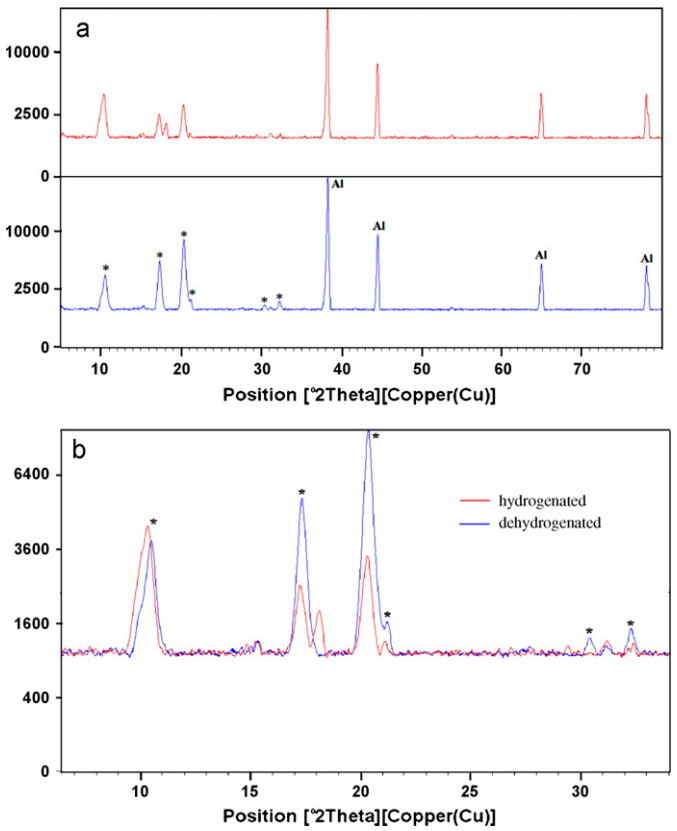

Fig. 3. X-ray powder diffraction of the desorbed and adsorbed $NaAlH_4$–C_{60} material. Identified by * in (a) is the Na_6C_{60} material as well as the presence of metallic aluminum as marked by the symbol, Al. A close-up overlap of the hydrogenated (red) and dehydrogenated (blue) material shows only subtle changes as the hydrogen adsorbs into the material. (For interpretation of the references to colour in this figure legend, the reader is referred to the web version of the article.)

reversibility reported for $NaAlH_4$ is instead likely due to the formation and hydrogen storage properties of a new material: sodium fulleride. XRD scans of the resultant dehydrogenated and hydrogenated material, shows a powder diffraction pattern which matches the known Na_6C_{60} fulleride and residual Al metal (Fig. 3) [26]. C_{60} appears to operate as a catalyst for the dehydrogenation of the sodium aluminum hydride ($NaAlH_4$). However, when sodium hydride (NaH) forms it reacts with the C_{60}, at a lower temperature than the NaH decomposition temperature. It appears that NaH is reacting and exchanging sodium with the C_{60} to form the previously reported sodium fulleride [26] and releasing hydrogen in the process. The destabilization mechanism for the complex hydride desorption is likely an electron withdrawing effect from the Na moiety contributing to the weakening of the metal–hydrogen bonding as described and predicted in previous computational work [1].

Without the reformation of any metal hydride species, as evidenced by the lack of a crystalline material in the XDR line pattern or characteristic peaks with FT-IR measurements (Fig. 4), the fulleride appears wholly responsible for the observed hydrogen storage reversibility (formation of AlH_3 requires $>10^5$ bar hydrogen overpressure). In addition, the rehydrided pattern indicates the aluminum remains metallic during the rehydriding treatments consistent with it functioning as a spectator material and not participating in hydrogen sorption. An examination of the XRD peak patterns (Figure 3b), demonstrates minor changes to the fulleride crystalline structure. The continued overall presence of Na_6C_{60} reflections between hydrogenated and dehydrgonated forms indicate the material maintains its general spatial structure, but the relative decrease in intensity of peaks at 17° and 20° (2θ) likely represents a deformation of structure due to hydrogen incorporation. High temperature and hydrogen overpressure during rehydrogenation may increase hydrogen content and could be reflected in diffraction characterization.

FT-IR spectroscopy of dehydrided and rehydrided Na_6C_{60} fulleride composite (Fig. 4) show the emergence of C–H stretching vibrations at $\sim$3000 cm^{-1} not present within a C_{60} standard exposed to identical absorption conditions with the Sieverts apparatus. The emergence of these C–H peaks are consistent with the formation of a hydrofullerene moiety as are the representative C–C stretching peaks at 1427 and 1181 cm^{-1}. The presence of these C–H stretches are evidence the hydrogen uptake observed is due to carbon–hydrogen bond formation of hydrofullerene rather than the rehydrogenation or reversal of the $NaAlH_4$ sorption mechanism [26]. In addition, these peaks shifts are similar to that observed for a Na_6C_{60}(THF) material which showed that the addition of the alkaline metal species changes the fullerenes normally high symmetry and causes a redistribution of electron density upon the fulleride formation [27].

3.2. $LiAlH_4$:C_{60} system

The $LiAlH_4$:C_{60} composite was synthesized with a molar ratio of 60:1 and was subject to the same hydrogen desorption/absorption conditions. The material was then characterized at various stages of the cycling process: as prepared, dehydrided and rehydrided. It has been reported that $LiAlH_4$ decomposes through three steps with

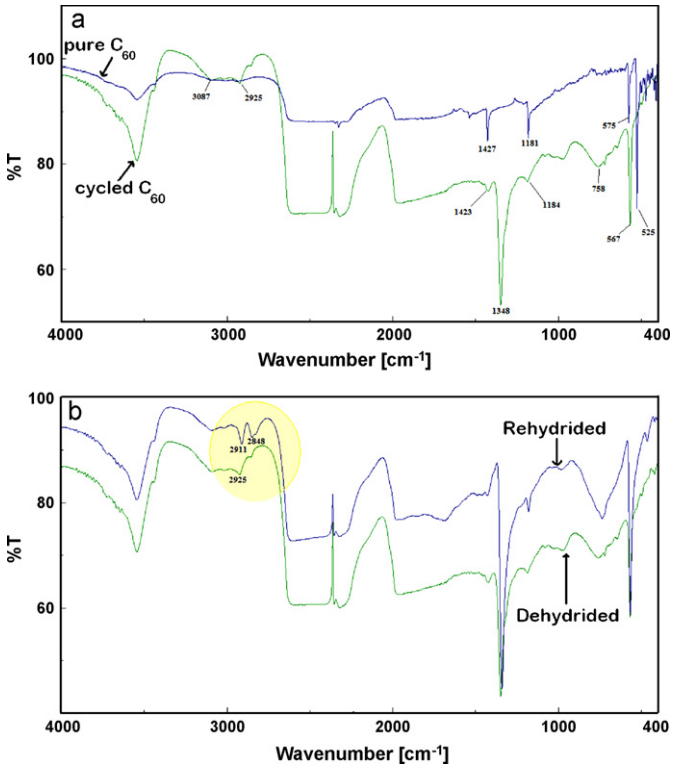

Fig. 4. FT-IR spectroscopy data for the (a) dehydrided (green) a comparison to an IR spectrum of pure C_{60} (blue) that was subjected to the same hydrogen cycling conditions (yet remained only as C_{60}). (b) Rehydrided Na_6C_{60} material (blue) is placed into comparison with the dehydrided material (green) showing the appearance of C–H stretches (highlighted in yellow) in the hydrogenated material. (For interpretation of the references to colour in this figure legend, the reader is referred to the web version of the article.)

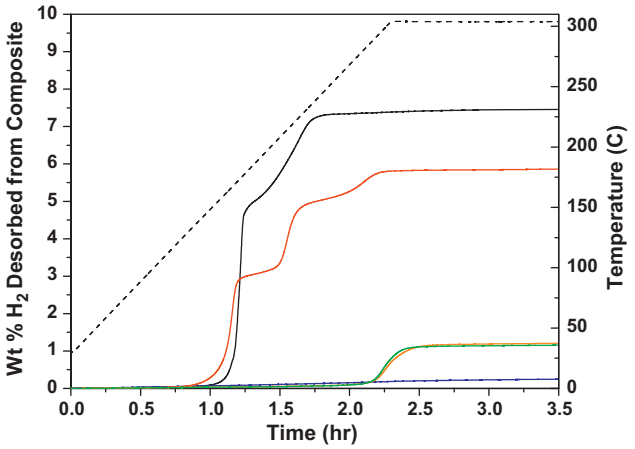

Fig. 5. TPD of pure $LiAlH_4$ (black—1st desorption, blue—2nd desorption), $LiAlH_4$:C_{60} (red—1st desorption, green—2nd desorption, orange—3rd desorption). Dashed line is the sample temperature. Heating rate was 2 °C/min. (For interpretation of the references to colour in this figure legend, the reader is referred to the web version of the article.)

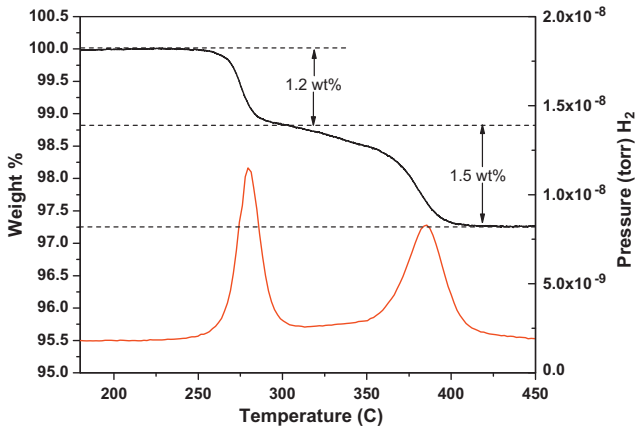

Fig. 6. TGA-RGA plot for $LiAlH_4$:C_{60} after the material was rehydrided twice and shows two distinct desorption events. The wt.% determined by the TGA is shown in black and the hydrogen signal from the RGA is shown in red. Heating rate was 2 °C/min. (For interpretation of the references to colour in this figure legend, the reader is referred to the web version of the article.)

5.3, 2.6, and 2.6 wt.% hydrogen released during each step respectively and is shown in reactions (4)–(6).

$$3LiAlH_4 \rightarrow Li_3AlH_6 + 2Al + 3H_2 \quad (4)$$

$$Li_3AlH_6 \rightarrow 3LiH + Al + 3/2H_2 \quad (5)$$

$$3LiH \rightarrow 3Li + 3/2H_2 \quad (6)$$

Reaction (4) occurs around 150 °C, reaction (5) occurs between 170–200 °C, and reaction (6) occurs at temperature above 680 °C [6,18,19,20]. However, due to the high temperatures need for reaction (6) to occur it is often disregarded and over looked since it is not practical for commercial use. This limits the available hydrogen content of $LiAlH_4$ to 7.9 wt.%.

TPD was used to determine the ability of the $LiAlH_4$:C_{60} material to reversibly store hydrogen through a series of desorption/absorption cycles and is shown in Fig. 5. The TPD of pure $LiAlH_4$ was also measured for comparison purposes. The first desorption of pure $LiAlH_4$ releases 7.5 wt.% in two distinct desorption events (reactions (4) and (5)) at 150 and 175 °C respectively. This desorbed material was then subject to hydrogen pressure and heat in an effort to recharge the sample. As expected, the second desorption of pure $LiAlH_4$ did not release any hydrogen. Unlike the pure complex hydride, the $LiAlH_4$:C_{60} composite shows *three* distinct desorption events indicating that all three desorption events (reactions (4)–(6)) occurred and released 5.9 wt.% hydrogen with respect to the weight $LiAlH_4$ and C_{60} combined. In addition the temperature at which the initial desorption event occurs is approximately 20 °C lower than in pure $LiAlH_4$.

Subsequent absorption and desorption cycles were performed and showed that the material can reversibly store 1.2 wt.% hydrogen. However, the release of hydrogen in the second and third desorption does not occur until ~260 °C. This data suggests that the material being regenerated during the absorption process is not $LiAlH_4$. Instead, the material being regenerated during the rehydrogenation is likely Li_x–C_{60}–H_y based on the temperature at which subsequent desorptions occur. Previous theoretical studies [28] of $Li_{12}C_{60}$ have predicted that the formation of Li_x–C_{60}–H_y is possible and could be the active hydrogen storage material formed during the subsequent cycling of the $LiAlH_4$:C_{60} material.

The rehydrided material was characterized using the TGA-RGA in order to confirm the amount of hydrogen released and is shown in Fig. 6. Interestingly, two distinct desorption events are observed, with the first occurring at ~260 °C (1.2 wt.%) and the other occurring at approximately 350 °C (1.5 wt.%). During the occurrence of both desorption events simultaneous hydrogen evolution is detected by the RGA. To ensure that the weight loss observed was not due to the degradation of the C_{60} as it reacts with $LiAlH_4$ the RGA was also set to monitor a variety of volatile carbon species but none were detected.

Any changes in the nature of the material during the desorption/absorption process was monitored using X-ray powder diffraction as is shown in Fig. 7. The as prepared sample shows a mixture of $LiAlH_4$ and C_{60}, while the dehydrided and rehydrided samples only show the presence of metallic aluminum and no $LiAlH_4$ or C_{60}. Unlike the $NaAlH_4$:C_{60} system described previously, no peaks are representative of a fulleride material. This could be due to the formation of an amorphous phase or incomplete formation of Li fulleride due to Li deficiency within the starting composite material. In either case, the crystalline nature of C_{60} within the composite is altered when subjected to the high temperatures and pressures of the cycling process. Despite the lack of crystalline structure measured by XRD, we believe a Li fulleride material is formed due to similar desorption/absorption and spectroscopic observations obtained for the Na fulleride system described above.

FT-IR was also used to monitor any changes in the material during the cycling process and is shown in Fig. 8. Fig. 8(a) compares C_{60}, pure $LiAlH_4$, and $LiAlH_4$:C_{60} as prepared. The as prepared sample closely resembles the spectrum of pure $LiAlH_4$ without any peaks associated with pure C_{60}. It is possible that the spectrum of $LiAlH_4$

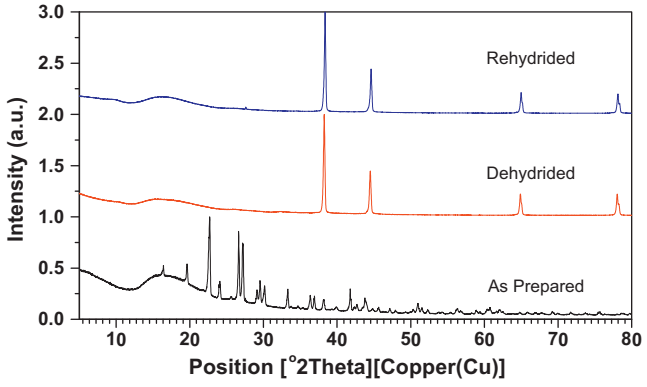

Fig. 7. XRD stack plot of the $LiAlH_4$:C_{60} at different stages of the absorption/desorption process. Both the dehydrided and rehydrided samples were analyzed after the 3rd cycle.

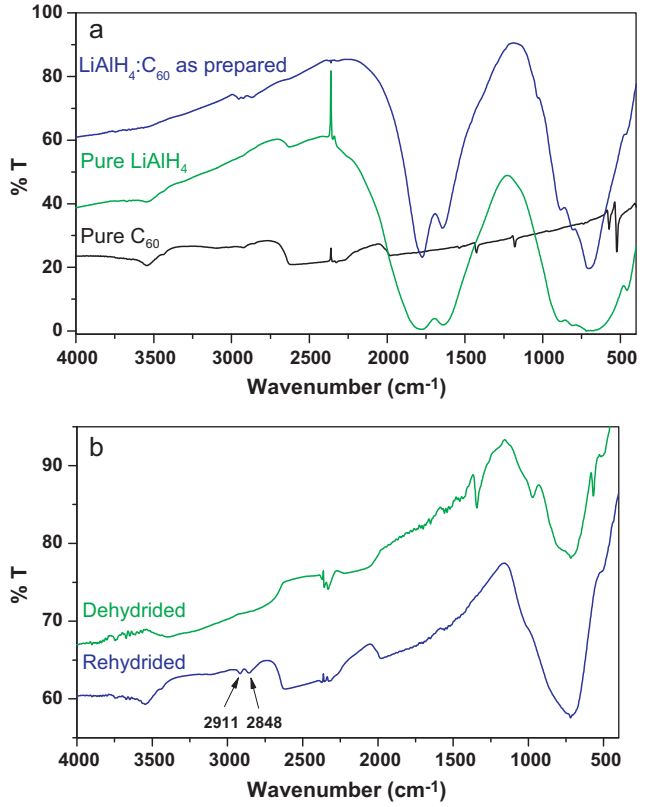

Fig. 8. FT-IR spectroscopy. (a) Black—pure C_{60}, Green—pure $LiAlH_4$, Blue—$LiAlH_4$:C_{60} as prepared. (b) Green—$LiAlH_4$:C_{60} dehydrided, Blue- Rehydrided. The peaks labeled are consistent with the formation of C–H bonds (2848 and 2911 cm^{-1}). (For interpretation of the references to colour in this figure legend, the reader is referred to the web version of the article.)

masks any of the C_{60} due to the large excess of $LiAlH_4$ relative to C_{60}. Fig. 8(b) compares the dehydrided and rehydrided $LiAlH_4$:C_{60} samples. Interestingly, the two peaks at 2911 and 2848 cm^{-1} are consistent with the formation of hydrogenated C_{60} [26,29]. The emergence of these C–H peaks are consistent with the formation of a hydrofullerene moiety similar to the $NaAlH_4$:C_{60} system. The presence of these C–H stretches are evidence that the observed partial hydrogen uptake is due to carbon–hydrogen bond formation of hydrofullerene [26,29] rather than the rehydrogenation or reversal of the $LiAlH_4$ sorption mechanism. The two desorption events observed in the TGA-RGA data could be due to the desorption of a Li fulleride with two different Li occupancy sites, occurring at 260 °C and at 350 °C. Li fullerides are known to be stable with Li_xC_{60} ($x \leq 28$) and the excess of Li is either a spectator, staying as LiH, or forms a Li_xC_{60} ($x > 28$) fulleride [30]. Regardless the temperatures required for absorption and desorption indicate the hydrogen is incorporated into the composite through chemisorption and not physisorption by bonding directly to either lithium or carbon atoms or both in the material. The role of the aluminum (if any) has not been determined as of yet in either system.

4. Conclusion

We have shown the unique ability of C_{60} to catalyze hydrogen desorption of complex metal hydrides, $NaAlH_4$ and $LiAlH_4$, and to subsequently form materials capable of reversible hydrogen desorption and absorption. However, when $NaAlH_4$ is dehydrogenated in the presence of C_{60}, Na_3AlH_6 was absent as an intermediate. Characterization of the cycled material indicates the alkali metal fullerides are responsible for the observed hydrogen absorption/desorption and are likely similar in structure and physical properties to hydrofullerenes. Unlike known hydrofullerene materials our results show fullerides with significantly lower temperatures of hydrogen desorption at 150 and 260 °C (Na_6–C_{60} and Li_{60}–C_{60}, respectively) compared to desorption temperatures of 450–600 °C for $C_{60}H_{18}$ [26]. In this work the formation of the Li fulleride is likely incomplete due to a surplus of starting $LiAlH_4$ and future work will explore optimum ratio, additional structural characterization, and the effects on hydrogen storage capacity. In addition, the hydrogen desorption of both systems does not appear to involve the formation of carbides or volatile hydrocarbons as determined by RGA, indicating a relative stable system for hydrogen storage. This study shows it is possible to dehydrogenate simple metal hydrides, once thought impractical for hydrogen storage (i.e. LiH and NaH), at lower temperature when mixed with carbon nanostructures such as C_{60}. We are continuing to investigate these systems and more results will be reported in due course.

Acknowledgement

J.T., D.K., M.W., and R.Z. thank the U.S. Department of Energy, Office of Basic Energy Science for funding. We would also like to thank Mr. Joseph Wheeler and Dr. Gregory Morgan for providing helpful assistance and support equipment.

References

[1] P.A. Berseth, A.G. Harter, R. Zidan, A. Blomqvist, C.M. Araujo, R.H. Scheicher, R. Ahuja, P. Jena, Nano Lett. 9 (2009) 1501.
[2] M.S. Wellons, P.A. Berseth, R. Zidan, Nanotechnology 20 (2009) 204022.
[3] B. Bogdanovic, M. Schwickardi, J. Alloys Compd. 253 (1997) 1.
[4] A. Andreasen, T. Vegge, A.S. Pedersen, J. Solid State Chem. 178 (2005) 3672.
[5] D. Blanchard, H.W. Brinks, B.C. Hauback, P. Norby, Mat. Sci. Eng. B 108 (2004) 54.
[6] J. Chen, N. Kuriyama, Q. Xu, H.T. Takeshita, T. Sakai, J. Phys. Chem. B 105 (2001) 11214.
[7] C. Cento, P. Gislon, M. Bilgili, A. Masci, Q. Zheng, P.P. Prosini, J. Alloys Compd. 437 (2007) 360.
[8] A.L. Dehouche, N. Grimard, J. Goyette, R. Chahine, Nanotechnology 16 (2005) 402.
[9] A. Zaluska, L. Zaluski, J.O. Strom-Olsen, J. Alloys Compd. 298 (2000) 125.
[10] D. Pukazhselvan, B.K. Gupta, A. Srivastava, O.N. Srivastava, J. Alloys Compd. 403 (2005) 312.
[11] J. Wang, A.D. Ebner, J.A. Ritter, J. Phys. Chem. B 110 (2006) 17353.
[12] J.B. Gao, P. Adelhelm, M.H. Verkuijlen, C. Rongeat, M. Herrich, P.J. van Bentum, O. Gutfleisch, A.P. Kentgens, K.P. de Jong, P.E. de Jongh, J. Phys. Chem. C 114 (2010) 4675.
[13] P. Adelhelm, J.B. Gao, M.H. Verkuijlen, C. Rongeat, M. Herrich, P.J. van Bentum, O. Gutfleisch, A.P. Kentgens, K.P. de Jong, P.E. de Jongh, Chem. Mat. 22 (2010) 2233.
[14] P. Adelhelm, K.P. de Jong, P.E. de Jongh, Chem. Commum. 45 (2009) 6261.
[15] A. Andreasen, J. Alloys Compd. 419 (2006) 40.
[16] V.P. Balema, V.K. Pecharsky, K.W. Dennis, J. Alloys Compd. 313 (2000) 69.
[17] X. Hu, M. Trudeau, D.M. Antonelli, Inorg. Chem. 47 (2008) 2477.
[18] L. Zaluski, A. Zaluska, J.O. Strom-Olsen, J. Alloys Compd. 290 (1999) 71.
[19] J. Block, A.P. Gray, Inorg. Chem. 4 (1965) 304.
[20] J.A. Dilts, E.C. Ashby, Inorg. Chem. 11 (1972) 1230.
[21] X.L. Wang, J.P. Tu, Appl. Phys. Lett. 89 (2006) 064101.
[22] Z. Tao, H. Geng, K. Yu, Z. Yang, Y. Wang, Mater. Lett. 58 (2004) 3410.
[23] N. Pierard, A. Fonseca, J.F. Colomer, C. Bossuot, J.M. Benoit, G. Van Tendeloo, J.P. Pirard, J.B. Nagy, Carbon 42 (2004) 1691.
[24] V.P. Balema, A.O. Pecharsky, V.K. Pecharsky, J. Alloys Compd. 307 (2000) 184.
[25] B. Bogdanovic, R.A. Brand, A. Marjanovic, M. Schwickardi, J. Tolle, J. Alloys Compd. 302 (2000) 36.
[26] S.M. Luzan, F. Cataldo, Y.O. Tsybin, A.V. Talyzin, J. Phys. Chem. C 113 (2009) 13133.
[27] S.N. Titova, G.A. Domrachev, S.Y. Khorshev, A.M. Obedkov, L.V. Kalakutskaya, S.Y. Ketkov, V.K. Cherkasov, B.S. Kaverin, K.B. Zhogova, M.A. Lopatin, V.L. Karnatsevich, E.A. Gorina, Phys. Solid State 46 (2004) 1365.
[28] Q. Sun, P. Jena, Q. Wang, M. Marquez, J. Am. Chem. Soc. 128 (2006) 9741.
[29] A.V. Talyzin, Y.M. Shulga, A. Jacob, Appl. Phys. A-Mater. Sci. Process. 78 (2004) 1005.
[30] M. Yasukawa, S. Yamanaka, Chem. Phys. Lett. 341 (2001) 467.